

Laminarization of Turbulent Boundary Layer on Flexible and Rigid Surfaces

Lucio Maestrello*

NASA Langley Research Center, Hampton, Virginia 23681-2199

An investigation of the control of turbulent boundary-layer flow over flexible and rigid surfaces downstream of a concave-convex geometry has been made. The concave-convex curvature induces centrifugal forces and a pressure gradient that affect the growth of the turbulent boundary layer. The favorable gradient is not sufficient to overcome the unfavorable one; thus, the net effect is a destabilization of the flow into Görtler instabilities. This study shows that control of the turbulent boundary layer and structural loading can be successfully achieved by using localized surface heating because the subsequent cooling and geometrical shaping downstream over a favorable pressure gradient are effective in laminarization of the turbulence. Wires embedded in a thermally insulated substrate provide surface heating. The laminarized velocity profile lowers the Reynolds number, and it reduces the structure loading. In the laminarization, the turbulent energy is dissipated by the molecular transport due to both viscous and conductivity mechanisms. Laminarization also reduces spanwise vorticity because of the longitudinal temperature gradient of the sublayer profile. The results demonstrate that the curvature-induced mean pressure gradient enhances the receptivity of the flow to a localized surface heating, a potentially viable mechanism to laminarize turbulent boundary-layer flow; thus, the laminarized flow reduces the response of the flexible structure and the resultant sound radiation.

I. Introduction

TURBULENT boundary-layer control is achievable experimentally by using a localized surface heating in a region of pressure gradient. Localized heating (in gas) leads to an increase in stability and the critical Reynolds¹ number. A new velocity profile is formed to adjust to the laminarized Reynolds number, which results in lower skin friction and structural loading. This adjustment occurs naturally in a high-speed flow and causes a hypersonic flow to become laminar and a hot jet to be quieter than a cold jet. The present experiment is designed to demonstrate the feasibility of flow stabilization for subsonic boundary-layer flow by means of a localized surface heating. Laminarization is achieved by the natural cooling of the flow downstream of a heated wire strip placed on a concave surface. The effectiveness of the technique depends on the pressure gradient, the temperature gradient, and the Reynolds number. The coupling between the heat flux and the streamwise pressure gradient influences the stability sufficiently to reverse the state of the flow from turbulent to laminar.

The shear flow over a concave surface is subject to centrifugal instability whose inviscid mechanism was given first by Reynolds¹ (1884) and Rayleigh² (1916) and in recent works by Narasimha and Sreenivasan,³ Hoffmann et al.,⁴ Hall,⁵ Floryan,⁶ Maestrello and El-Hady,⁷ and Bayliss et al.⁸ These works have indicated that the flow over a concave surface is potentially unstable, resulting in two- and three-dimensional disturbances, whereas the flow over a convex surface is stabilizing. The overall effect of the surface curvature on the flow cannot be predicted a priori; it depends on the parameters of the flow and initial disturbance.

In the past decade, the study of nonlinear and chaos control has attracted much attention.^{9–15} Recently, investigations have shifted to spatiotemporal systems to control pattern formation including turbulence. Turbulence remains an extremely important problem

in engineering and in other fields of science and is an example of spatiotemporal chaos. The deterministic and chaotic responses need to be distinguished from stochastic behavior. Typically, random behavior can arise in a number of ways, but actually, the behavior is the result of deterministic chaos that appears random because of the lack of sufficient information about initial starting condition.^{9,10,14} Vibration control using an actuator for stabilizing panel vibration satisfying a nonlinear beam equation is studied by Chow and Maestrello¹⁶ with a perturbation technique. The vibration control principle can also be applied to other problems such as nonlinear wave propagation and flow stability and control. A potentially less restricted method of control is by passive surface heating¹⁷; Maestrello and Ting¹² analyzed this problem by using the method of matched asymptotes as a “triple-deck” problem. This analysis confirmed that a small amount of localized surface heating can excite local disturbances that increase the momentum near the wall and reduce the displacement thickness and, as a result of downstream cooling, can laminarize the turbulent flow.

In this paper, the effect of a local surface heating and the curvature-induced pressure gradient on the growth of the turbulent boundary layer is studied. In particular, with the use of a wire strip on the concave portion of the surface, the flow behavior resulting from an imposed steady localized heating is investigated. The boundary layer is turbulent, nearly two dimensional in the mean; three-dimensional centrifugal instability is created by the largest eddies present in the flow approaching the concave portion of the surface. Centrifugal effects can be categorized into three types: 1) change in the turbulent structure induced by the wall curvature, 2) generation of longitudinal vortices, and 3) effect of the longitudinal vortices on turbulent structure. Over the concave portion of the surface, vortex cells are triggered by the interaction between the centrifugal instability and the level of fluctuations created by the eddies in the boundary layer.

Structural vibration and the resulting sound radiation can also be controlled by suppressing waves on the structure rather than by controlling the boundary layer itself. One method uses the so-called rubber wedges designed to attenuate waves incident and reflecting from the boundaries. Laboratory testing using rubber wedges at low flow speed and flight testing on a Boeing 727 airplane at Mach number 0.85 and altitude of 930 m show 15 and 8 dB, respectively, of broadband acoustic power reduction. The added mass for the modified boundaries was approximately 30% of the panel weight.^{18,19}

The analysis is concerned with passive control by localized surface heating, and the experiment begins with measurements of local fluctuations and mean velocities, followed by the distribution of the

Received 27 February 2001; revision received 15 February 2002; accepted for publication 9 August 2002. Copyright © 2002 by the American Institute of Aeronautics and Astronautics, Inc. No copyright is asserted in the United States under Title 17, U.S. Code. The U.S. Government has a royalty-free license to exercise all rights under the copyright claimed herein for Governmental purposes. All other rights are reserved by the copyright owner. Copies of this paper may be made for personal or internal use, on condition that the copier pay the \$10.00 per-copy fee to the Copyright Clearance Center, Inc., 222 Rosewood Drive, Danvers, MA 01923; include the code 0001-1452/03 \$10.00 in correspondence with the CCC.

*Scientist, Aerodynamics, Aerothermodynamics, and Acoustic Competency, Mail Stop 463. Associate Fellow AIAA.

average temperature cooling downstream of the heating wire, then the sequence of Görtler vortices during laminarization stages, and finally the fluctuations and mean velocity of the uncontrolled and the controlled boundary layer. The analysis of control by surface heating is given in Sec. II. Section III describes the configuration geometry and instrumentation. Results on the control of Görtler instability and the laminarization of the boundary layer and the structural response are described in Secs. IV.A and IV.B, respectively.

II. Flow Analysis of Localized Surface Heating and Downstream Cooling

Flow analysis of localized surface heating was developed by Maestrello and Ting¹² based on the pioneering work of Liepmann et al. at the California Institute of Technology.¹⁷ They demonstrated experimentally that localized periodic active surface heating can be used to excite controlled boundary-layer disturbances either to cancel or to trip the Tollmien–Schlichting waves. A heuristic argument was presented¹² to explain the equivalence between heat flux and effective normal velocity at the wall because the coupling between the thermal and mechanical effects is provided by the dependence of viscosity on temperature. The governing flow equations are presented as an indicator of the important parameters. The equations are not used to calculate trends for localized surface heating on turbulent flow over a concave–convex surface.

Localized surface heating in air alters the growth of the flow instability by subsequent cooling downstream. As a result, the flow stability is increased by the modifications of the velocity and pressure distribution. The analysis must begin with the energy equation, even for incompressible flow. The problem deals with a change in thermal boundary conditions, which in turn creates a disturbance field in the boundary layer. The thermal sublayer is assumed to be much less than the local boundary layer and is analyzed by the integral equation method for steady two-dimensional incompressible flow.

Qualitative effects on the stabilization of the boundary layer due to localized heating with subsequent downstream cooling were obtained for air because the viscosity μ increases with temperature T , that is,

$$\frac{d\mu}{dT} > 0$$

Surface heating with subsequent downstream cooling changes the velocity profile due to the dependence of viscosity on temperature. An extra term $(d\mu/dT)(\partial T/\partial y)(\partial u/\partial y)$ appears on the right-hand side of the momentum equation for an incompressible boundary layer, where y is the coordinate normal to the surface. Here μ , T , u , and y are nondimensional quantities, and u is the velocity. For the experimental results (Sec. IV), thin wire strips are heated electrically by an electric current with frequency ω . With the power proportional to $\cos 2\omega t$, the temperature of a heating strip T_w can be written as $T_0 + 2T_1 \cos 2\omega t$, where T_0 is the adiabatic wall temperature. The temperature derivation becomes

$$\Delta T = T_w - T_0 = T_1 + T_1 \cos 2\omega t \quad (1)$$

and is composed of a steady term T_1 , an oscillatory term with amplitude T_1 , and frequency 2ω . It is clear that both the steady and the oscillatory terms can contribute to boundary control but that they play different roles. In this paper we shall carry out the first step, the effect of steady disturbance. We shall use the method of matched asymptotics to relate the temperature, velocity, and pressure disturbances to the local surface heating. It is well known that a change of boundary condition creates a disturbed flowfield in the boundary layer. The local disturbed field can be subdivided into three layers known as the triple deck governed by different sets of approximate equations for each deck and joined to each other by the matching conditions. The triple-deck analysis has been applied to many problems in boundary layers with sudden changes of wall velocity or external pressure.^{20,21} The present problem differs from those because we have a sudden change in thermal boundary condition.¹² The formulation of the lower portion of the triple deck, the viscous layer, is outlined in this section. The second step is the use of an

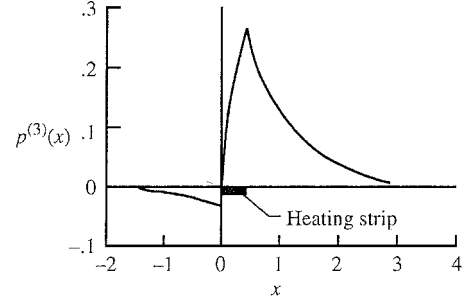


Fig. 1 Pressure distributions induced by steady surface heating.

active external force that was recently applied to control synchronization on structure forced by turbulent boundary layer and sound and to control screech tone.^{14,15,22}

The analysis begins with the energy equation for an incompressible flow. The governing equations in dimensionless quantities for $u^{(2)}(x, y, t)$, $v^{(3)}(x, y, t)$, $T^{(1)}(x, y, t)$, and $p^{(3)}(x, t)$, corresponding to velocities u and v , temperature T , and pressure p for the lower deck, are shown as follows, with the superscripts indicating the order of the perturbation in the expansion schemes and identifying the corresponding power of the expansion parameter ε , where $\varepsilon = (Re)^{-1/8}$:

$$u_x^{(2)} + v_y^{(4)} = 0 \quad (2)$$

$$u_t^{(2)} + \beta y u_x^{(2)} + \beta v_y^{(4)} = -p_x^{(3)}(x, t) + u_{yy}^{(2)} + \Lambda \beta T_y^{(1)} \quad (3)$$

$$T_t^{(1)} + \beta y T_x^{(1)} = (Pr)^{-1} T_{yy}^{(1)} \quad (4)$$

$$p_x^{(3)}(x, t) = \frac{1}{\pi} \int_{-\infty}^{\infty} \frac{A_\xi(\xi, t) d\xi}{x - \xi} \quad (5)$$

where Λ is equal to $d \ln(\nu)/d \ln(T)$, Pr is the Prandtl number at T_0 , and β is the slope of the velocity profile at the wall. The variation of viscosity with temperature in the momentum equation, because it is associated with the pressure gradient, becomes the mechanism that effectively alters the turbulent boundary layer, that is, the forcing term $\Lambda \beta T_y^{(1)}$. For the Blasius profile, β equals 0.33206. Notice the $\Lambda \beta T_y^{(1)}$ dependency of u and T due to the forcing term for $u^{(2)}$, $v^{(4)}$, and $p^{(3)}$. The term $A_x(x, t)$ is equal to $\partial A(x, t)/\partial x$ and

$$A(x, t) = \beta^{-1} u^{(2)}(x, y \rightarrow \infty, t)$$

The pressure gradient $p_x^{(3)}(x, t)$ is a Hilbert transform of $A_x(x, t)$ (Ref. 12). On the heating wire, it is assumed that

$$T^{(1)} = (T_w - T_0)/\varepsilon T_0 = 1 + \cos \omega_0 t$$

This analysis provides the solution of the velocity and pressure distributions. If the frequency is finite, $\mathcal{O}(1)$, the full unsteady analysis has to be carried out. In the usual linearized incompressible equations, the unsteady term and the last term in Eq. (2) are absent; the energy equation for temperature is not needed for the solution of the velocity disturbances. A numerical example of the pressure distribution $p^{(3)} = -(\Delta p/\rho U_0^2 \varepsilon^3)$ is plotted in Fig. 1 with $\Delta x = 0.75$ and $\Delta T = 100^\circ\text{C}$. (ΔT is the temperature of the heating strip above the plate temperature.) Inspection of Fig. 1 indicates that the pressure distribution decreases slightly below zero as x increases ($x < 0$). As x increases over the heating strip, the pressure distribution increases rapidly to reach a maximum at the end of the strip. In the downstream of the strip, it decreases rapidly as x increases. Heating of the air destabilizes over the heating strip because $d\mu/dT$ is greater than zero, but it stabilizes downstream of the heating strip due to subsequent and geometrical shaping downstream over the favorable pressure gradient. The overall values for temperature change ΔT , Prandtl number Pr , and Λ are given in Table I and used to evaluate Fig. 1. The contribution of the steady-quasi-steady terms depends on the size of ΔT and $d\mu/dT$, whereas the unsteady terms depend on frequencies and phases of the heat source.

Table 1 Values for temperature change ΔT , Prandtl number Pr , and Λ

$\Delta T, ^\circ\text{C}$	Pr	Λ
10	0.72	1.535
100	0.72	16.52

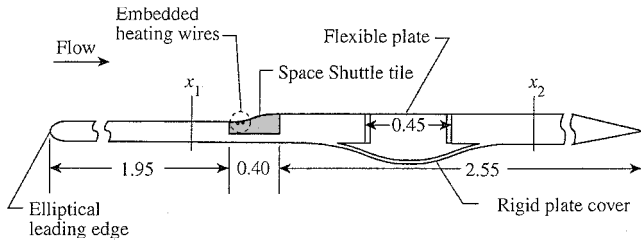


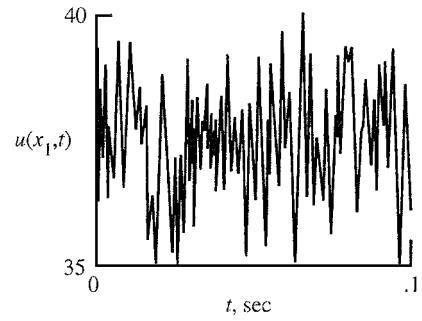
Fig. 2 Experimental model; dimensions in meters.

III. Configuration Geometry and Instrumentation

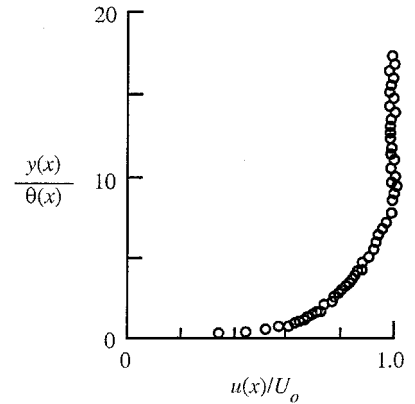
The experiment is conducted in an open-circuit wind tunnel with a 38.1 by 38.1 cm test section at a speed of 36.6 m/s on a plate 4.8 m long (Fig. 2). A portion of the plate is concave and a portion is convex with flat regions upstream and downstream (Fig. 2). Upstream, the plate features an elliptic leading edge with a thickness of 2.54 cm, and downstream it features a trailing edge with controllable angle flap. The concave-convex portion is described by a seventh-degree polynomial with the first three derivatives continuous at both ends. This degree of smoothness is designed to prevent singularities from being generated at the points where the surface becomes flat. This geometry was selected to illustrate the effect of curvature-induced pressure gradient flow and flexible structure stability. The concave portion has an adverse pressure gradient, and the mean flow decelerates, whereas downstream the curvature becomes convex and produces a favorable pressure gradient and the flow accelerates. The surface contains a thermally insulated substrate (space shuttle tile). The flow behaviors caused by imposed steady heating from two wires in the concave portion were investigated. The wires are nickel-chromium strips with resistance about 4 Ω/m . The wires are held in position under tension during the heating and cooling cycles. The power supply operates in a direct-current mode in a manner similar to that of a previous experiment using leading-edge heating on a flat plate.¹³ The heater current and voltage are continuously monitored, and they are used to determine the total power input during the control cycle. The surface temperature downstream of the heating wires is measured by a line of thermocouples placed along the side-wall corner of the tunnel test section. Downstream of the concave-convex curvature, the surface is flat, and a flexible aluminum plate is located 40 cm from the curvature. The plate, 45 \times 20.3 \times 0.08 cm, with clamped edges is mounted flush with the surface and is used to study the structural loading. The rest of the surface is rigid. A hot-wire probe, accelerometer, wall pressure transducer, temperature sensors, and infrared thermography²³ were used to evaluate the flow and structure response. The infrared thermography technique is a nonintrusive method to investigate the changes of the Görtler vortices with temperature gradient. The wind-tunnel geometry, flow quality, freestream turbulent level, and background noise permit a study of the laminarization control problem of a turbulent boundary layer at low speed.

IV. Experimental Results

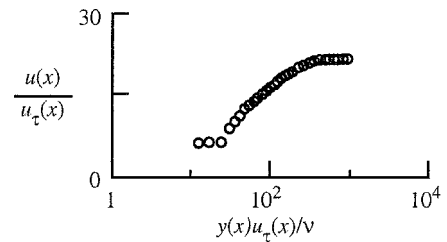
The mean velocity profiles, perturbation velocity, and the infrared thermogram of the developing vortices over the concave-convex surface are evaluated. The uncontrolled boundary layer is turbulent upstream and downstream of the curved surface. The concave surface has a destabilizing effect because it increases the levels of Reynolds shear stress and turbulent energy and enhances the turbulent mixing, whereas the convex surface has a stabilizing effect on Reynolds shear stresses and turbulent energy level; turbulent mixing has a decreasing level compared with an equivalent straight shear layer flow.



a) Velocity fluctuation



b) Mean velocity profile



c) Frictional velocity profile

Fig. 3 Turbulent boundary layer at location x_1 .

A. Görtler Instability Perturbation Velocity, Mean Velocity, and Laminarization of Turbulence

The perturbation velocity $u(x, t)$ vs t , the mean velocity profile $y(x)/\theta(x)$ vs $u(x)/U_0$, and the frictional velocity $u(x)/u_\tau(x)$ vs $y(x)u_\tau(x)/\nu$ at location x_1 are shown in Fig. 3, where $u(x, t)$ is the local fluctuation velocity, y is the coordinate, θ is boundary-layer displacement thickness, $u(x)$ is mean local velocity, U_0 is freestream velocity, $u_\tau(x)$ is the local frictional velocity, and ν is kinematic viscosity. The location of x_1 is 40 cm upstream of the curvature. A wind-tunnel condition is chosen from the calibration runs based on flow, vibration, and noise quality. From the mean velocity profiles and perturbation velocity, one can deduce that the uncontrolled boundary layer is turbulent at freestream velocity, $U_0 = 36.6$ m/s, and Reynolds number, $Re_\theta(x_1) = 2010$. The frictional velocity profiles are comparable with the standard wall law for the turbulent boundary layer over a flat plate.

The choice of the geometry in Fig. 2 permits laminarization of the boundary layer downstream of a concave-convex surface by localized heating on the concave portion of the surface. The average wall temperature distributions T_w/T_0 downstream of the heating wires decay exponentially with distance to cause the flow to laminarize, as shown in Fig. 4. The upper curve in Fig. 4 is the temperature ratio used to trip transition from a turbulent state, and the lower curve is the temperature ratio used to maintain a laminar flow. In this ratio, T_w is the wall temperature downstream of the heating wires, and T_0 is the ambient temperature of the wind-tunnel wall. Figures 5a–5f show the infrared thermogram vorticity patterns over the concave-convex curvature. Figures 5a–5f show the temperature

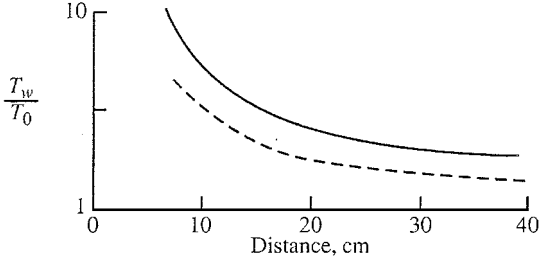


Fig. 4 Average surface temperature downstream of heating: —, ratio to trip laminar boundary layer and - - -, ratio to maintain laminar boundary layer.

of the heating elements required to induce transition and to maintain laminar flow. The Görtler vortices originate from the concave portion of the surface, and they become stabilized over the convex portion of the surface as the temperature decays with distance. Stability of the vortices is indicated by the increase in wavelength and a sudden increase in size as the number of vortices reduces. The temporal stages toward laminarization are related to the thermoconductivity gradient of the surface and flow characteristics. Distinct features in the time sequences of the vorticity pattern are shown in each step (Fig. 5). During control stages, the heat flux through the wire is gradually increased until the reversion from a turbulent to a laminar state is established. Then the amount of heat flux is reduced by 25% equivalent to 200 W after establishing laminarization of

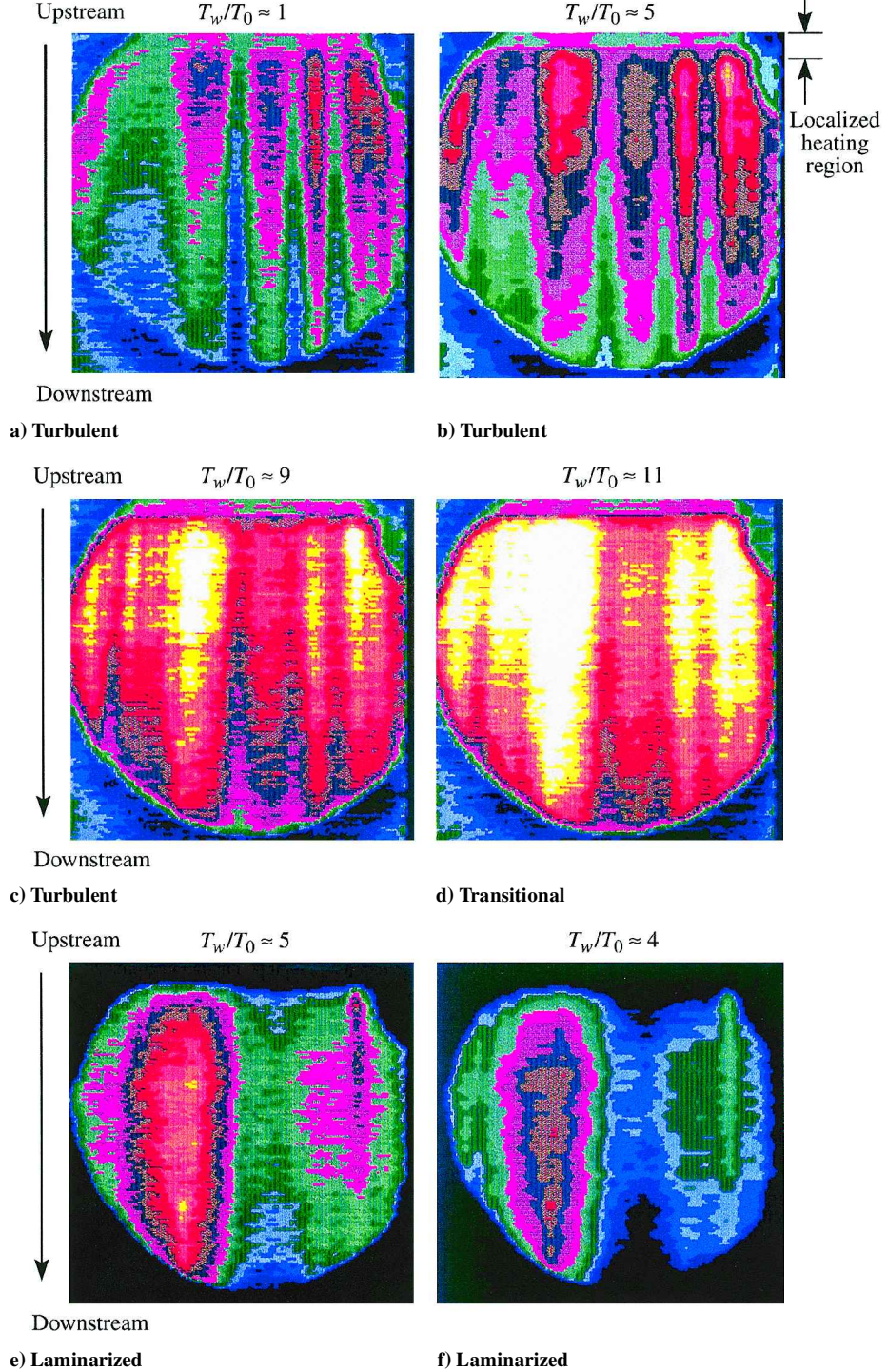


Fig. 5 Time sequence of Görtler vortices over concave-convex curvature during laminarization stages.

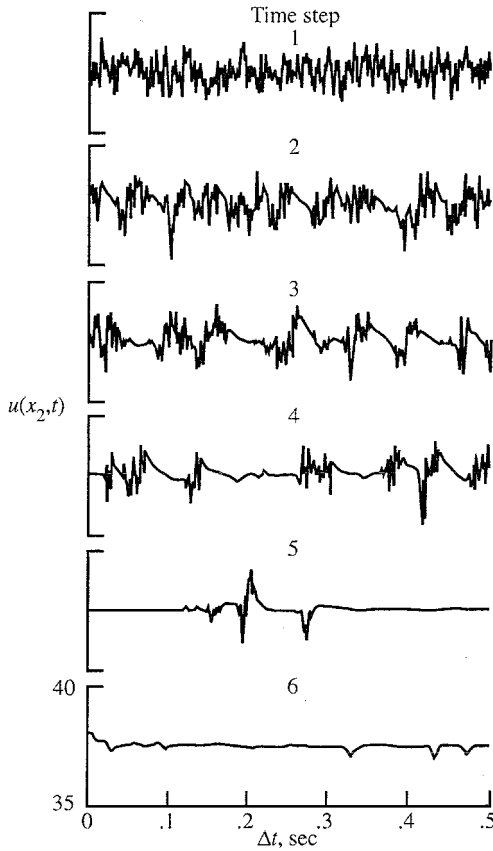
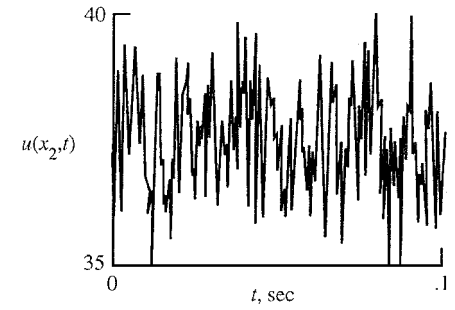


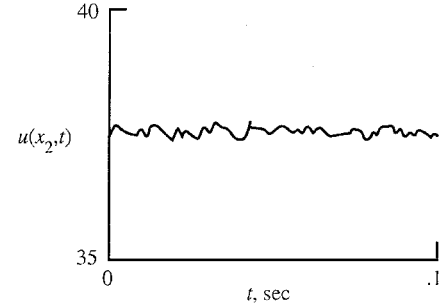
Fig. 6 Fluctuation velocity for successive time steps Δt from turbulent to laminarized state at location x_2 .

the turbulent boundary layer. The analysis in Sec. II can provide the guidelines. The Görtler patterns stretch downstream over the convex portion with increased stability as the temperature decreases with distance (Fig. 5a). The perturbations of the flow over the heating wires amplify a region of an unfavorable pressure gradient and then the perturbation decays due to cooling in the region of a favorable gradient. This reversion in the amplification is due to both geometrical shaping of the curvature profile and surface cooling with downstream distance. Figure 5a also indicates that the changing pattern is not two dimensional. In Figs. 5b–5d, the temperature of the wire increases. (Red indicates the higher and blue the lower temperature.) The decrease in wall temperature with downstream distance causes drastic changes in vorticity; the boundary layer laminarizes in the process. In the laminarized state only two large vortices remain; the spatial change is an indication of stabilization (Figs. 5e and 5f). The vorticity is concentrated in the core surrounded by a large-scale motion with small-scale vortices embedded within; it is possible to recognize successive changes as the wire temperature increases.

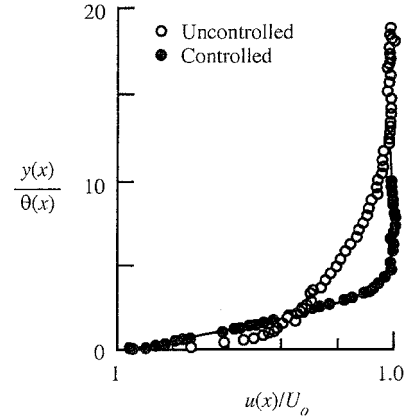
The temporal sequences of the velocity perturbations, before, during, and after laminarization, are shown in Fig. 6 at x_2 located 40 cm downstream of the flexible panel. Six successive time-step intervals Δt are shown, from the turbulent state, time step 1, to the laminar state, time step 6. The features seen during transition are like the features seen in a turbulent spot, that is, time step 5. The perturbations in time steps 2–4 have a higher amplitude than in the turbulence in step 1 and should be interpreted as the envelope of all of the possible types of disturbance amplification. The process of laminarization also indicates a change in Reynolds numbers from $Re_\theta(x_2) = 2728$ in the turbulent state to $Re_\theta(x_2) = 983$ in the laminarized state. These changes in perturbation velocity and mean velocity profiles are shown in Fig. 7. The mean profile (Fig. 7c) changes from turbulent in the initial stage to laminarized in the final stage resembling the Blasius profile. The perturbation velocity changes also indicate laminarization of the turbulence. The displacement thickness Reynolds number $Re_\theta(x_2)$ equal to 2728 corresponds to $Re(x)$ based on plate length at x_2 of over 1×10^6 , which certainly seems to be a practical value for a turbulent boundary layer over



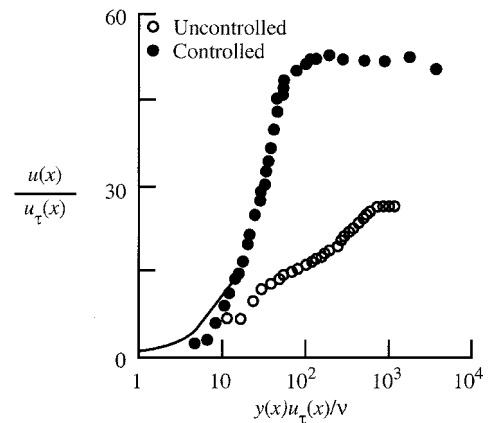
a) Uncontrolled velocity fluctuation



b) Controlled velocity fluctuation



c) Uncontrolled and controlled mean velocity profile



d) Uncontrolled and controlled frictional velocity profile

Fig. 7 Turbulent and laminarized boundary layer at location x_2 .

a flat plate. This $Re(x)$ corresponds to about midrange the data shown in Schlichting's Fig. 21.2 (Ref. 24). This is the turbulent flow that is laminarized. That the laminarized flow is approximately one-third as thick as the corresponding turbulent flow also agrees with Schlichting's Fig. 21.2 if such flow could be attained at that $Re(x)$. During the control stages, as heat on the wire strips increases, the boundary layer at x_1 becomes intermittently turbulent with an oscillation in $Re_\theta(x_1)$ between 5 and 15% from its original value.

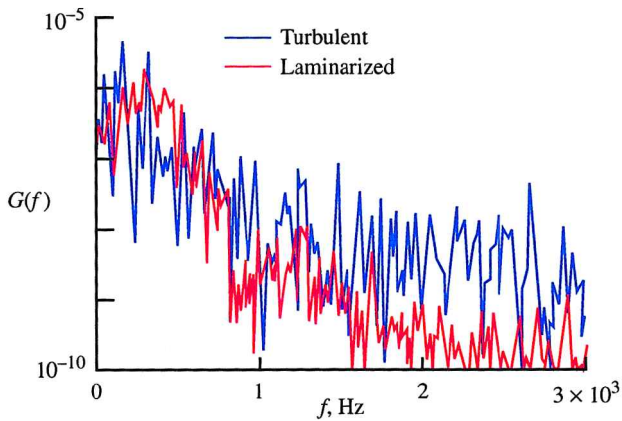


Fig. 8 Response of the panel structure forced by turbulent and laminarized boundary layers.

The pressure gradient in the control region of the heating wires and downstream is essential to maintain the coupling between the thermal gradient and the sublayer because coupling the heat input with the flow at zero pressure gradient is virtually impossible. This important feature "pressure gradient" is indicated on the right-hand side of the momentum equation (2) with viscosity as a function of temperature. The rate of cooling with distance is the stabilizing mechanism; as a result, the critical Reynolds number increases. There is no bounded limit on how far laminarization can be extended because the stability increases with the increasing ratio between the local heat flux and the thermal conductivity and the temperature. The whole laminarization process looks like transition to turbulence in reverse as can be observed from a fixed point.

B. Panel Structure Response and Control

The response of the panel is induced by the convecting boundary-layer loading, both turbulent and laminar. The static pressure difference across the panel is 2.5 kg/m^2 , and the static deflection is less than the panel thickness. The pressure difference has an effect on the structural response. The response is measured by an accelerometer at the panel center.

The normalized power spectral density $G(f)$ of the acceleration for the turbulent and the laminarized boundary-layer loading is shown in Fig. 8. No attempt is made to measure the spatiotemporal response. The spectrum is dominated by the lower frequencies, an expected result for low-speed boundary-layer loading. The controlled spectrum has a lower amplitude than the uncontrolled one; their differences increase with frequency (Fig. 8). At the low frequencies, the reduction in power is approximately 7 dB, at high frequencies, more than 10 dB. Laminar boundary-layer loading reduces the structural response with respect to the turbulent boundary layer. The acoustic background noise of the facility did not permit measurement of the acoustic power (radiated) by the panel. From the response, one expects that the acoustic spectrum will be dominated by the low frequencies with a lower level for the laminarized boundary-layer loading than for the turbulent one. Larger differences in structural response are expected for higher speed flow because the convected waves of the panel dominate the response over a wider bandwidth.

V. Conclusions

An investigation of the control of the turbulent boundary layer over rigid and flexible surfaces downstream of a concave-convex geometry was made. Heating was applied at the concave surface. Pressure gradient forces crucially influence the control of turbulence. The Görtler spatial pattern that extends over the curved surface is marked by changes of vorticity over time. The physical significance is that the cooling pattern over a favorable pressure gradient is a gain

in stability of the flow. Laminarization reduces the Reynolds number, spanwise vorticity, wall pressure fluctuations, and structural loading. The effectiveness of the technique depends on the pressure gradient, the temperature gradient, and the Reynolds number. The coupling between the heat flux and the streamwise pressure gradient influences the stability sufficiently to reverse the state of the flow. The drawback of using such a control system is that the power required can be higher than the power reduction in the system response.

References

- Reynolds, O., "The Two Manners of Motion of Water," *Proceedings of Royal Institution of Great Britain*, Vol. 11, 1884, pp. 44–52.
- "413. On the Dynamics of Revolving Fluids," *Scientific Papers by Lord Raleigh, Proceedings of the Royal Society of London, Series A: Mathematical and Physical Sciences*, Vol. 93, No. A648, 1916, pp. 148–154.
- Narasimha, R., and Sreenivasan, K. R., "Relaminarization of Fluid Flows," *Advances in Applied Mechanics*, Vol. 19, 1979, pp. 221–308.
- Hoffmann, P. H., Muck, K. C., and Bradshaw, P., "The Effect of Concave Surface Curvature on Turbulent Boundary Layers," *Journal of Fluid Mechanics*, Vol. 161, 1985, pp. 371–403.
- Hall, P., "The Nonlinear Development of Görtler Vortices in Growing Boundary Layer," *Journal of Fluid Mechanics*, Vol. 193, 1988, pp. 243–266.
- Floryan, J. M., "On the Görtler Instability of Boundary Layer," *Progress in Aerospace Sciences*, Vol. 28, No. 3, 1991, pp. 235–271.
- Maestrello, L., and El-Hady, N. M., "Radiation and Control of Sound From Evolving Wave Packet on a Concave-Convex Surface," *AIAA Journal*, Vol. 29, No. 6, 1991, pp. 880–887.
- Bayliss, A., Maestrello, L., Parikh, E., and Turkel, E., "Numerical Simulation of Boundary-Layer Excitation by Surface Heating/Cooling," *AIAA Journal*, Vol. 24, No. 7, 1986, pp. 1095–1101.
- Ott, E., Grebogi, C., and Yorke, J. A., "Controlling Chaos," *Physical Review Letters*, Vol. 64, No. 11, 1990, pp. 1196–1199.
- Pecora, L. M., and Carroll, T. L., "Driving Systems with Chaotic Signals," *Physics Review A*, Vol. 44, No. 4, 1991, pp. 2374–2383.
- Ditto, W. L., Spano, M. L., and Lindner, J. F., "Technique for the Control of Chaos," *Physica D*, Vol. 86, No. 9, 1995, pp. 198–211.
- Maestrello, L., and Ting, L., "Analysis of Active Control by Surface Heating," *AIAA Journal*, Vol. 23, No. 7, 1985, pp. 1038–1045.
- Maestrello, L., and Grosveld, F. W., "Transition Control of Instability Waves over an Acoustically Excited Surface," *AIAA Journal*, Vol. 30, No. 3, 1992, pp. 665–670.
- Maestrello, L., "Controlling Vibrational Chaos of a Curved Structure," *AIAA Journal*, Vol. 39, No. 4, 2001, pp. 581–589.
- Maestrello, L., "The Influence of Initial Forcing on Non-Linear Control," *Journal of Sound and Vibration*, Vol. 239, No. 4, 2001, pp. 873–883.
- Chow, P. L., and Maestrello, L., "Vibrational Control of a Non-Linear Elastic Panel," *International Journal of Non-Linear Mechanics*, Vol. 36, 2001, pp. 709–718.
- Liepmann, H., Brown, G. L., and Nosenchuck, D. M., "Control of Laminar-Instability Waves Using a New Technique," *Journal of Fluid Mechanics*, Vol. 118, May 1982, pp. 187–200.
- Maestrello, L., "Use of Turbulent Model To Calculate the Vibration and Radiation Responses of a Panel with Practical Suggestions of Reducing Sound Level," *Journal of Sound and Vibration*, Vol. 5, No. 3, 1967, pp. 407–448.
- Baht, W. V., and Wilby, J. F., "Interior Noise Radiation by an Airplane Fuselage Subjected to Turbulent Boundary Layer Excitation and Evaluation of Noise Reduction Treatments," *Journal of Sound and Vibration*, Vol. 18, No. 4, 1971, pp. 449–464.
- Stewartson, K., "Multistructured Boundary Layer on Flat Plates and Related Bodies," *Advances in Applied Mechanics*, Vol. 14, 1974, pp. 145–239.
- Smith, F. T., "On the High Reynolds Number Theory of Laminar Flow," *Journal of Applied Mathematics*, Vol. 28, 1982, pp. 207–281.
- Maestrello, L., "Active Control of Panel Oscillation Induced by Accelerated Boundary Layer and Sound," *AIAA Journal*, Vol. 35, No. 5, 1997, pp. 796–801.
- Carlomagno, G. M., and De Luca, L., "Infrared Thermography Applications in Convective Heat Transfer," *Flow Visualization V*, edited by R. Reznicek, Hemisphere, New York, 1990, pp. 843–848.
- Schlichting, H., *Boundary Layer Theory*, 6th ed., translated by J. Kestin, McGraw-Hill, New York, 1968, p. 600.

H. M. Atassi
Associate Editor